Contribution to the structural study of $Rb_3Ln(PO_4)_2$ materials (Ln=La, Ce, Pr, Nd, Sm, Eu, Gd and Tb) by vibrational spectroscopy

L. Rghioui*, L. Benarafa, R. Khaoulaf, A. El Hajji, L. Guennoun, M. Serghini Idrissi

Laboratory of Spectroscopy, Molecular Modeling, Materials, Nanomaterials, Water and Environment, (LS3MN2E-CERNE2D), Department of Chemistry, Faculty of Sciences, Mohammed V University in Rabat, P.O.Box. 1014, Agdal-Rabat, Morocco

In this work, structural studies of phosphates with general formula $Rb_3Ln(PO_4)_2$ (Ln=La, Ce, Pr, Nd, Sm, Eu, Gd and Tb) were performed by vibrational spectroscopy. These materials were synthesized by a solid-state reaction. They crystallized in monoclinic system with space group $P2_1/m$. A complete vibrational study by infrared and Raman spectroscopy was carried out. These phosphates exhibited a monoclinic $P2_1/m \rightarrow$ trigonal P-3m1 phase transition which was studied by Raman spectroscopy.

Keywords: Infrared, spectroscopy, Raman, phase transition, monoclinic, trigonal

INTRODUCTION

Inorganic compounds with general formula $M_3Ln(XO_4)_2$ (M=K, Rb; Ln=rare earth element and X=P,V) have attracted much attention due to their applications as phosphors, lasers or solid state lighting materials [1-11]. For instance, Kloss *et al.* studied the luminescence phenomenon in $K_3Eu(PO_4)_2$ and $Rb_3Eu(PO_4)_2$. They also studied the $Rb_3Ln(PO_4)_2$ (Ln=La, Eu and Gd) and $K_3Eu(PO_4)_2$ compounds by vibrational spectroscopy, but this study is incomplete [1]. The luminescence properties of Ce-activated $K_3Lu(PO_4)_2$ were analyzed by Wisniewski *et al.* [2]. They concluded that the luminescence of this material is dominated by the d-f emission bands of Ce^{3+} and that the Ce-activated $K_3Lu(PO_4)_2$ is a promising fast and efficient scintillator. Using high-temperature oxide-melt solution calorimetry, Ushakov *et al.* [3] have determined the formation enthalpies for $K_3Ln(PO_4)_2$ (Ln= Sc, Y, Ce, Nd, Gd, Dy, Ho, Lu) compounds and for $A_3Lu(PO_4)_2$ phosphates with A= Rb or Cs. Using high-temperature X-ray diffraction and differential scanning calorimetry, the authors followed the phase transition phenomenon exhibited by these compounds. Farmer *et al.* [4] have studied the structure of $K_3Lu(PO_4)_2$ phosphate as a function of temperature by X-ray and powder neutron diffraction. Two lower-temperature phases were characterized for this compound at 230K and 130K. Crystals of $Rb_3Ln(PO_4)_2$ (Ln= La,…, Lu and Y) have been synthesized by Tisdale *et al.* [5]. Their structures were resolved and determined using X-ray diffraction. The fluorescence emission spectra of $Rb_3Eu(PO_4)_2$ and $Rb_3Tb(PO_4)_2$ were also studied [5]. Luminescence characteristics of $K_3Lu(PO_4)_2$ doped with Pr^{3+} were studied by Ivanovskikh *et al.* [6]. The authors showed that these compounds are promising optical materials for scintillation applications and that high concentration of Pr^{3+} ions (5%) is found to be favorable for the stabilization of the monoclinic phase. Pelczarska *et al.* [7] synthesized $Rb_3La(PO_4)_2$ undoped and doped with Eu^{3+} ions. The characterization of these two compounds by X-ray diffraction showed that they exhibit a monoclinic structure in the $P2_1/m$ space group by isotypy with $K_3Nd(PO_4)_2$ phosphate [7].The authors measured the life time of $^5D_0$ excited state at 77K and they found it to be 4 ms. The $4f^15d^1\rightarrow 4f^2$ interconfigurational transitions of the Pr^{3+} ions were studied by Carrasco *et al.* [8] in $K_3Lu_{1-x}Y_x(PO_4)_2$ doped with 1% of Pr^{3+}. The authors concluded that the substitution of Lu by Y causes a blue shift of the $4f^15d^1\rightarrow 4f^2$ emission.

The present work is a structural study by vibrational spectroscopy on compounds with general formula $Rb_3Ln(PO_4)_2$ (Ln= La, Ce, Pr, Nd, Sm, Eu, Gd and Tb). It is a continuation of our investigations on phosphates, vanadates and arsenates with general formula $M_3Ln(XO_4)_2$ and $M_2M'Ln(XO_4)_2$ (Ln= rare earth and X= P, V, As) [12-22]. To our knowledge, no detailed vibrational studies have been carried out for $Rb_3Ln(PO_4)_2$ (Ln= La, Ce, Pr, Nd, Sm, Eu, Gd and Tb) phosphates.

* To whom all correspondence should be sent:
E-mail: *rghiouilotfi@gmail.com*

EXPERIMENTAL

Syntheses of $Rb_3Ln(PO_4)_2$ samples (Ln= La,…,Tb) were carried out using conventional solid-state reaction techniques. Powdered crystalline samples were prepared from a stoichiometric mixture of Rb_2CO_3, Ln_2O_3 (CeO_2, Pr_6O_{11}, Tb_4O_7) and $(NH_4)_2HPO_4$. The mixture was ground in an agate mortar and heated at 120°C overnight, at 400°C for 24h and at 600°C for 24h to expel the decomposition products NH_3, H_2O and CO_2 respectively. A final treatment at 1000°C for 48h was realized to obtain the pure product.

The recording of the X-ray diffraction patterns was carried out using a D5000 Siemens diffractometer equipped with Bruker DIFFRAC plus EVA software, Bragg-Brentano geometry with a θ-2θ goniometer and a copper anode K_α (λ =1.5406Å). The angular domain in 2θ is 10-60°.

Infrared spectra were recorded using two types of spectrometers:

 - A Fourier transform spectrometer type Perkin Elmer 1600. The spectral resolution is 4 cm^{-1} over the whole range 4000-450 cm^{-1}.

 - A Fourier transform spectrometer I.F.S. 113V type Bruker (700-100 cm^{-1}). The resolution is estimated at 2 cm^{-1}.

The spectra were obtained after pelleting in potassium bromide KBr (4000-450 cm^{-1}) or in polyethylene $(C_2H_4)_n$ (700-100 cm^{-1}). The pellets in KBr were made from 1 to 2 mg of the product in 100 mg of KBr and those in $(C_2H_4)_n$ were obtained from 2.5 mg of the product in 50 mg of polyethylene.

Raman spectra were recorded with a DILOR RT30 spectrometer equipped with two types of krypton- and argon-ionized laser Spectra-Physics 2020. Several radiations were used: 647.1 nm, 514.5 nm, 488 nm and 457.9 nm. The resolution is 1 to 2 cm^{-1}. The compounds were examined in the form of powders.

RESULTS AND DISCUSSION

X-ray diffraction study

The powder X-ray diffraction analysis of $Rb_3Ln(PO_4)_2$ phosphates with Ln=La,…, Tb allowed us to conclude that these compounds crystallize in monoclinic system with space group $P2_1/m$ by isotypy with $K_3Nd(PO_4)_2$ phosphate. Our results are in very good agreement with those published by Tisdale *et al.* [5].

The crystal structure of $K_3Nd(PO_4)_2$ phosphate was described by Hong and Chin [23]. The main structural units of this compound are isolated PO_4 tetrahedra and NdO_7 decahedra. There are two types of PO_4 tetrahedra. The first, denoted P(1), shares two oxygen atoms with the same neodymium atom and shares the other two oxygen atoms with two different neodymium atoms (Figure 1). The second, denoted P(2), shares three oxygen atoms with three different neodymium atoms; the fourth oxygen atom is bound to a potassium atom (Figure 1) [23].

The unit lattice parameters of $Rb_3Ln(PO_4)_2$ compounds were calculated and their values are given in Table 1.

Figure 2 gives the variation of the unit cell volume of $Rb_3Ln(PO_4)_2$ compounds as a function of the radius of the rare earth ion. As it is shown in this figure, the volume of the cell regularly decreases when atomic number increases in accordance with the decrease in the ionic radii of the rare earth elements. The values of the ionic radii of the rare earth ions are taken from the Shannon tables [24] with coordination equal to 7.

Table 1. Unit lattice parameters of $Rb_3Ln(PO_4)_2$ compounds

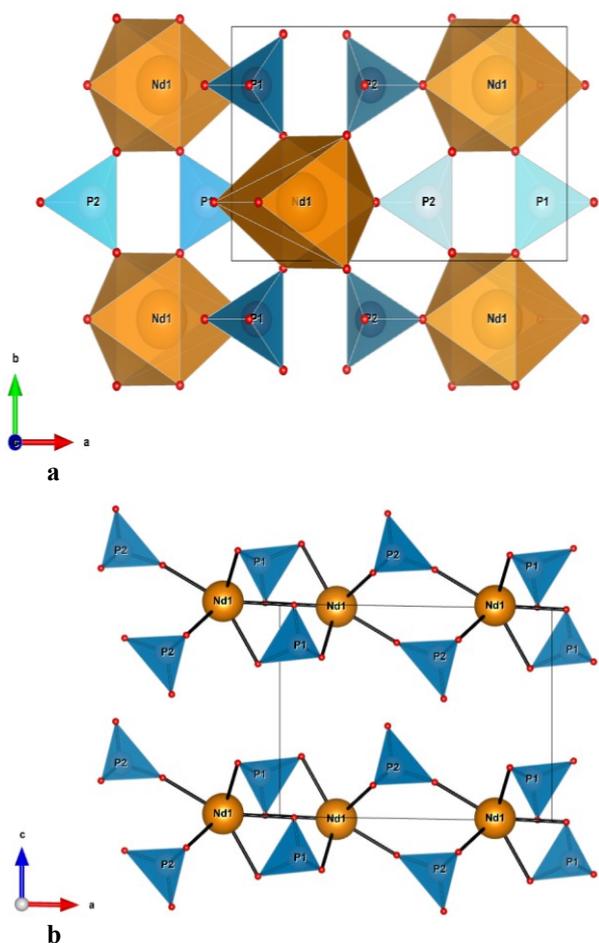| $Rb_3Ln(PO_4)_2$	La	Ce	Sm	Eu	Gd	Tb
r (Å)	1.10	1.07	1.02	1.01	1.00	0.98
(a±0.006)(Å)	9.881	9.832	9.784	9.761	9.752	9.743
(b±0.004)(Å)	5.843	5.840	5.805	5.784	5.762	5.753
(c±0.005)(Å)	7.850	7.832	7.790	7.753	7.724	7.705
(β±0.02) (°)	90.50	90.47	90.23	90.20	90.10	90.08
(V±1) (Å^3)	453	450	442	438	434	432

Fig. 1. Projection of $K_3Nd(PO_4)_2$ structure on:
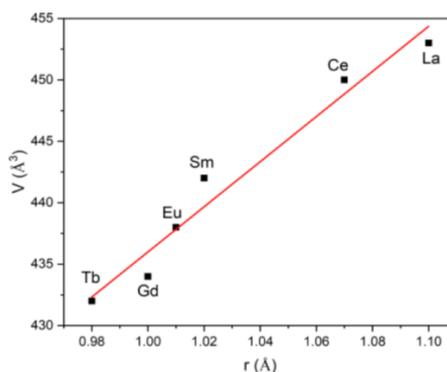
a-(001) plan; b-(010) plan [23].

Fig. 2. Evolution of the unit cell volume with the radius of the rare earth ion.

Raman and infrared studies

$Rb_3Ln(PO_4)_2$ phosphates (Ln= La,…, Tb) have a monoclinic structure type $K_3Nd(PO_4)_2$ (space group $P2_1/m$ (C_{2h}^2) and Z=2 [23]). The Ln, Rb and P atoms occupy 2e (C_s) sites and the oxygen atoms are distributed between the 2e (C_s) and the general 4f (C_1) positions. The structure, considered as ionic, is formed by the PO_4^{3-} groups and the Rb^+ and Ln^{3+} cations. So, the separation between internal and external vibrations is possible. The factor group analysis was performed using a correlation method [25]. For the internal vibrations of each PO_4^{3-}, the correlation between molecular group T_d, site group C_s and factor group C_{2h} is given in Table 2-a. The external modes correspond to the rotational movements of PO_4^{3-} and to the translation movements of PO_4^{3-}, Rb^+ and Ln^{3+}. Table 2-b gives the correlation between site group C_s and factor group C_{2h} for these external modes.

Table 2-a. Correlation scheme for internal modes of PO_4^{3-} ions

Internal modes	T_d		C_s		C_{2h}
ν_1	A_1	$\rightarrow$	A'	$\rightarrow$	$A_g + B_u$
ν_2	E	$\rightarrow$	A' + A''	$\rightarrow$	$A_g + B_u + B_g + A_u$
ν_3	T_2	$\rightarrow$	2A' + A''	$\rightarrow$	$2A_g + 2B_u + B_g + A_u$
ν_4	T_2	$\rightarrow$	2A' + A''	$\rightarrow$	$2A_g + 2B_u + B_g + A_u$

Table 2-b. Correlation scheme for external modes of PO_4^{3-}, Rb^+ and Ln^{3+} ions

		C_s		C_{2h}
External modes	Rotation of PO_4^{3-}	A' + 2A''	$\rightarrow$	$A_g + B_u + 2B_g + 2A_u$
	Translation of PO_4^{3-}	2A' + A''	$\rightarrow$	$2A_g + 2B_u + B_g + A_u$
	Translation of Rb^+ and Ln^{3+}	2A' + A''	$\rightarrow$	$2A_g + 2B_u + B_g + A_u$

According to Table 2-a, for each type of PO_4^{3-} ion, the symmetric stretching vibration ν_1 with A_1 symmetry in the molecular group (T_d) gives one vibration in the site group (C_s) with A' symmetry and two vibrations in the factor group C_{2h} with A_g and B_u modes. The symmetric bending ν_2 with E symmetry in the molecular group is decomposed into two vibrations in the site group with A' and A'' modes and into four vibrations in the factor group ($1A_g$, $1B_g$, $1A_u$ and $1B_u$). Each vibration of T_2 type in the molecular group gives rise to three vibrations in the site group ($2A'$ and $1A''$) and six vibrations in the factor group ($2A_g$, $2B_u$, $1B_g$ and $1A_u$).

The 36 internal vibrations of the PO_4^{3-} groups are subdivided in the C_{2h} factor group as follows:

Γ_{vib} (PO_4^{3-})= $12A_g+6B_g+6A_u+12B_u$.

The 12 rotations of PO_4^{3-} groups are given by the following representation:

Γ_R (PO_4^{3-})= $2A_g+4B_g+4A_u+2B_u$.

The distribution of the 33 translations of PO_4^{3-}, Rb^+ and Ln^{3+} is given as follows:

Γ_T (PO_4^{3-}, Rb^+, Ln^{3+})= $12A_g+6B_g+5A_u+10B_u$ with $\Gamma_{ac} = A_u+2B_u$.

The A_g and B_g modes are Raman-active while the A_u and B_u modes are infrared-active.

Raman and infrared spectra of the monoclinic $Rb_3Ln(PO_4)_2$ phosphates (Ln=La,…,Tb) are presented in Figures 3-a and 3-b,respectively. A notable similarity is observed for all infrared and Raman spectra. This confirms that these compounds are isostructural. In addition, these spectra are also very similar to those of $K_2RbLn(PO_4)_2$ (Ln= La,…, Dy) and $K_3Ln(PO_4)_2$ (Ln= La,…, Yb) phosphates which have the same symmetry (monoclinic, space group $P2_1/m$ and Z=2) [12,17]. The peak positions and their assignments are given in Tables 3 and 4.

The interpretation of the spectra can be made on the basis we used for the monoclinic $K_2RbLn(PO_4)_2$ (Ln= La,…, Dy) and $K_3Ln(PO_4)_2$ (Ln= La,…, Yb) phosphates [12,17]. Thus, we can assign the Raman peaks observed between 1081 and 960 cm^{-1} to the PO_4^{3-} asymmetric stretching vibration ν_3 with T_2 symmetry in molecular group T_d and (A_g, B_g) modes in factor group C_{2h} (Table 3-a). This vibration appears in the infrared spectra between 1100 and 965 cm^{-1} with A_u and B_u symmetry species in factor group (Table 4-a).

The Raman peaks located between 928 and 960 cm^{-1} are attributed to the PO_4^{3-} symmetric stretching vibration ν_1 with A_1 symmetry in molecular group

T_d and A_g symmetry in factor group C_{2h} (Table 3-a). The corresponding bands in the infrared spectra are observed between 928 and 955 cm^{-1} with B_u symmetry in C_{2h} (Table 4-a) [12,17].

The asymmetric deformation modes of PO_4^{3-} group ν_4 with T_2 symmetry in T_d gave rise to six Raman peaks between 605 and 552 cm^{-1} type A_g and B_g and five infrared bands between 602 and 540 cm^{-1} type A_u, B_u in C_{2h} (Tables 3-a and 4-a) [12,17].

The Raman and infrared bands observed in the range 480- 390 cm^{-1} are attributed to the symmetric deformation vibrations ν_2 with E symmetry in T_d (Tables 3-a and 4-a) [12,17].

Below 250 cm^{-1}, we observed Raman and infrared bands attributed to external vibrations. They correspond to the libration modes of the PO_4^{3-} groups and to the translation modes of the PO_4^{3-}, Rb^+ and Ln^{3+} ions (Tables 3-b and 4-b) [12,17]. The Raman peaks observed between 190 and 245 cm^{-1} are assigned to the rotational modes of PO_4^{3-} with A_g and B_g symmetry. The corresponding bands in the infrared spectra are observed between 138 and 244 cm^{-1} with A_u and B_u symmetry. The translational modes of PO_4^{3-} ions are located between 150 and 190 cm^{-1} in the Raman spectra and between 100 and 130 cm^{-1} in the infrared spectra. The bands observed in the spectra at wave numbers below 100 cm^{-1} are attributed to the translation modes of lanthanide and Rb^{3+} ions. The separation between these modes seems difficult.

The vibration wavenumbers of phosphates $Rb_3Ln(PO_4)_2$ (Ln= La,..., Tb) show an evolution by change of the rare earth element. Thus, as an example we present on Figure 4 the evolution of the ν_1 mode according to the radius of the Ln^{3+}ion. A linear shift of this mode towards high frequencies was observed as the radius of the lanthanide decreases. This displacement can be explained by the fact that the replacement of a rare earth by another of smaller size leads to a decrease in the unit cell volume (Table 1 and Figure 2). Consequently, a strengthening of the P-O bonds took place, resulting in an increase in the frequency of vibration.

The slight difference between the slopes of the two straight lines is to be linked to the existence of two types of tetrahedra $P(1)O_4$ and $P(2)O_4$ in the crystal lattice [23].

Table 3-a. Raman peak positions (cm^{-1}) and their assignments (internal modes)

La	Ce	Pr	Nd	Sm	Eu	Gd	Tb	Attribution M.G.(T$_d$)	F.G.(C$_{2h}$)
1081	1081	1081	1081	1081	1081	1081	1081		A$_g$
1038	1042	1045	1048	1052	-	1058	1058		A$_g$
1013	1013	1013	1013	1014	1014	1015	1016	ν$_3$(T$_2$)	A$_g$
1002	996	994	994	991	-	-	-		B$_g$
976	976	979	979	981	990	986	986		A$_g$
960	960	960	962	964	969	971	971		B$_g$
952	953	955	956	959	960	960	960	ν$_1$(A$_1$)	A$_g$
928	929	929	930	931	932	932	932		A$_g$
598	600	601	601	603	603	605	605		A$_g$
583	583	584	583	584	584	584	585		B$_g$
573	573	573	573	573	573	575	576	ν$_4$(T$_2$)	A$_g$
568	568	569	568	568	569	569	570		A$_g$
560	558	561	560	560	561	561	562		B$_g$
554	554	554	554	553	552	552	552		A$_g$
442	443	445	447	450	451	452	453		A$_g$
417	417	419	418	423	421	421	422	ν$_2$(E)	B$_g$
413	413	414	414	416	415	415	416		B$_g$

M.G.: molecular group, F.G.: factor group

Table 3-b. Raman peak positions (cm^{-1}) and their assignments (external modes)

La	Ce	Pr	Nd	Sm	Eu	Gd	Tb	Attribution in M.G.	Attribution in F.G.
216	220	224	225	234	237	240	245		B$_g$
207	210	214	-	216	217	217	-	Rotation of PO$_4^{3-}$	A$_g$
-	-	-	210	-	212	214	215		A$_g$
190	192	194	195	200	202	204	205		B$_g$
182	184	-	-	187	190	191	194		A$_g$
173	173	181	180	175	178	179	179	Translation of PO$_4^{3-}$	B$_g$
163	166	169	170	172	174	-	-		A$_g$
154	155	157	156	159	159	160	157		A$_g$
133	135	136	136	139	139	140	141		A$_g$
116	117	116	116	117	-	-	-		A$_g$
108	109	109	109	111	112	112	111		A$_g$
100	101	101	101	103	104	104	104		B$_g$
92	94	95	95	98	99	98	98		A$_g$
85	87	87	87	90	-	89	90	Translation of Rb^{3+} and lanthanides	B$_g$
77	77	77	77	79	77	76	-		A$_g$
68	69	69	69	71	72	71	71		A$_g$
60	60	60	60	68	-	-	60		A$_g$
50	50	50	50	50	50	-	-		A$_g$
44	44	45	43	46	46	-	44		A$_g$
37	37	39	36	39	39	-	38		A$_g$

M.G.: molecular group, F.G.: factor group

Table 4-a. Infrared peak positions (cm^{-1}) and their assignments (internal modes)

La	Ce	Pr	Nd	Sm	Eu	Gd	Tb	M.G.(T_d)	F.G.(C_{2h})
-	-	1085	1085	1091	1097	1100	1100		
1069	1071	1070	1069	1071	1075	1075	1075		
-	-	-	-	1052	1055	1057	1060	$\nu_3(T_2)$	A_u, B_u
1005	1004	1005	1003	996	1000	1000	998		
965	965	967	967	967	980	975	974		
947	948	952	950	953	955	955	955	$\nu_1(A_1)$	B_u
-	-	928	930	928	928	928	928		
590	593	595	595	600	600	602	602		
-	-	-	-	-	-	-	587		
579	580	580	581	581	583	582	582	$\nu_4(T_2)$	A_u, B_u
570	570	570	570	573	573	574	573		
545	544	543	543	542	545	541	540		
457	460	466	469	470	472	472	473		
411	412	412	412	413	413	413	413	$\nu_2(E)$	A_u, B_u
403	403	405	403	402	401	402	402		
395	395	395	395	394	394	394	395		

M.G.: molecular group, F.G.: factor group

Table 4-b. Infrared peak positions (cm^{-1}) and their assignments (external modes)

La	Ce	Pr	Nd	Sm	Eu	Gd	Tb	Attribution
-	218	220	226	234	238	240	244	
208	193	196	194	202	206	206	204	Rotation of PO_4^{3-}
172	172	174	174	180	184	186	186	(A_u, B_u)
138	138	138	136	138	139	139	138	
124	126	128	126	134	131	130	131	
112	112	114	115	130	116	120	-	Translation of PO_4^{3-}
104	105	106	109	116	110	110	-	(A_u, B_u)
91	92	92	94	109	94	96	98	
79	78	78	78	94	78	78	78	Translation of Rb^{3+} and lanthanides
74	74	-	74	74	78	-	-	(A_u, B_u)
70	-	-	69	74	-	-	-	
64	64	64	-	68	68	-	-	
58	58	61	62	61	57	65	65	
-	-	54	54	54	54	58	54	

M.G.: molecular group, F.G.: factor group

Study of the phase transition by Raman spectroscopy

Tisdale *et al.* [5] followed the structural evolution of Rb₃Ln(PO₄)₂ phosphates as a function of temperature. They showed that these compounds exhibit a phase transition from the monoclinic (P2₁/m) to the trigonal (P-3m1) space group. The transition temperature depends on the nature of the rare earth ion and the trigonal phase is of glaserite type [5].

For our part, we have examined the evolution of our materials symmetry with temperature using differential thermal analysis technique. The increase in temperature causes a phase transition. Table 5 gives the values of the phase transition temperatures for the compounds studied. These values are very close to that published by Tisdale *et al.* [5].

By comparison with M₂CsLn(PO₄)₂ phosphates (M = K, Rb) and Rb₂KDy(VO₄)₂ and Cs₁.₅₂K₁.₄₈Gd(VO₄)₂ vanadates which have a glaserite structure [16, 18, 22], we can conclude that in Rb₃Ln(PO₄)₂ phosphates (at high temperature), the Rb atoms occupy two sites of symmetry, C₃ᵥ and D₃d, respectively, the rare earth element is logged in a site of D₃d symmetry, while the phosphorus atom is located in a site of C₃ᵥ symmetry.
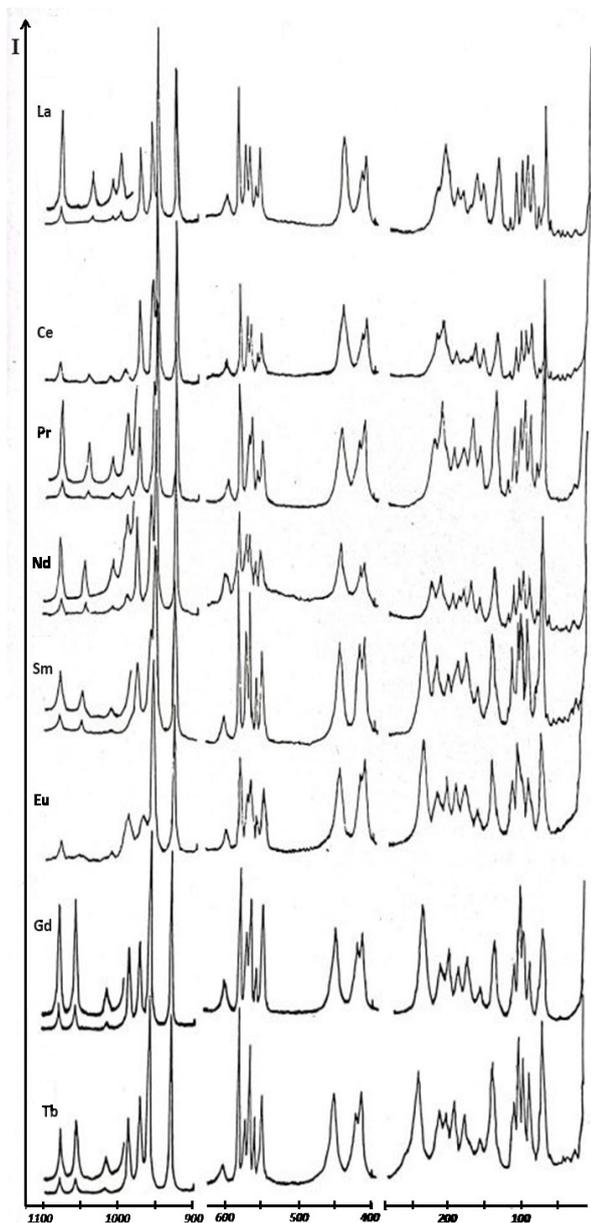
Fig. 3-a. Raman spectra of Rb$_3$Ln(PO$_4$)$_2$ phosphates (Ln=La,…, Tb)
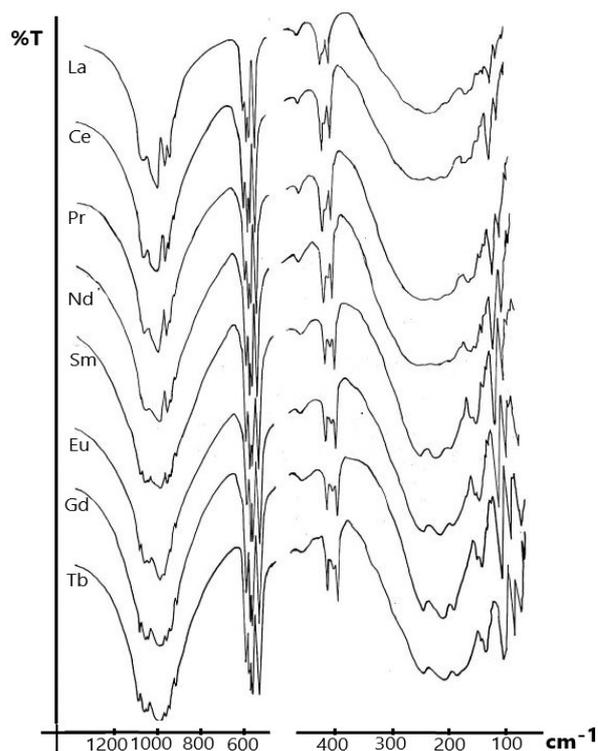

Fig. 3-b. Infrared spectra of Rb$_3$Ln(PO$_4$)$_2$ phosphates (Ln=La,…, Tb)

The 18 internal vibrations of the PO$_4^{3-}$ groups are subdivided as follows:

Γ_{vib} (PO$_4^{3-}$)= 3A$_{1g}$+3A$_{2u}$+3E$_g$+3E$_u$

The 6 rotations of PO$_4^{3-}$ groups are given by the following representation:

Γ_R (PO$_4^{3-}$)=A$_{1u}$+A$_{2g}$+E$_g$+E$_u$

The distribution of the 15 translations of PO$_4^{3-}$, Rb$^+$ and Ln^{3+} is given as follows:

Γ_T (PO$_4^{3-}$, Rb$^+$, Ln^{3+})= 2A$_{1g}$+3A$_{2u}$+2E$_g$+3E$_u$ with Γ_{ac} = A$_{2u}$+E$_u$

The A$_{1g}$ and E$_g$ modes are Raman-active while the A$_{2u}$ and E$_u$ modes are infrared-active. The A$_{2g}$ and A$_{1u}$ modes are inactive.

Table 5: Values of the temperature transition for Rb$_3$Ln(PO$_4$)$_2$ phosphates

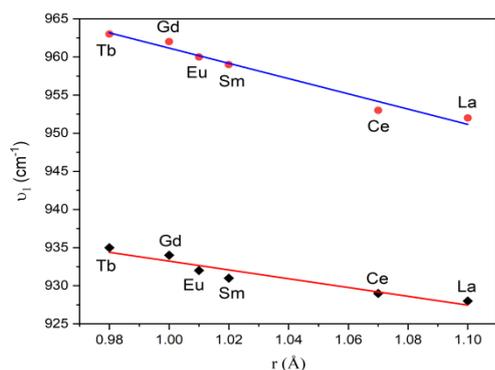| Ln	La	Ce	Pr	Nd	Sm	Eu	Gd	Tb
T(°C)	1080	990	940	845	680	520	380	90

Fig.4. Evolution of ν_1 mode with the radius of the rare earth

The Raman spectrum of Rb$_3$Eu(PO$_4$)$_2$ was recorded between ambient temperature and 700°C. Figure 5 shows the Raman spectra at ambient temperature and at 600°C. The change observed in the spectrum at 600°C indicates that the phosphate Rb$_3$Eu(PO$_4$)$_2$ exhibits a phase transition at high temperature. In addition, the Raman spectrum at 600°C is very similar to those of K$_2$CsLn(PO$_4$)$_2$ and Rb$_2$CsLn(PO$_4$)$_2$ phosphates which have a glaserite type symmetry (trigonal, P-3m1 space group)[18]. This confirms that Rb$_3$Eu(PO$_4$)$_2$ phosphate has a glaserite type structure at high temperature.
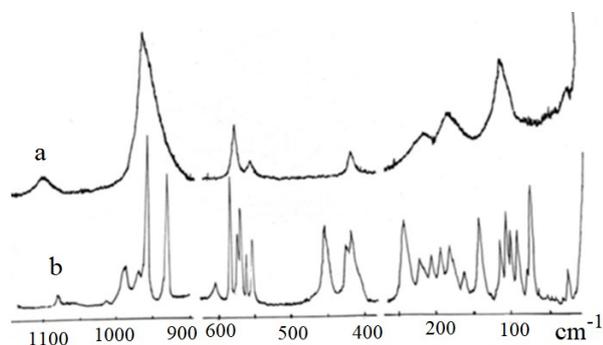

Fig. 5. Raman spectra of Rb$_3$Eu(PO$_4$)$_2$ at 600°C (a) and at ambient temperature (b)

The spectrum recorded at 600°C shows two broad peaks at 956 cm^{-1} attributed to the PO$_4^{3-}$ symmetric and asymmetric stretching vibrations (ν_1 and ν_3) and at 1100 cm^{-1} due to the ν_3 mode. Between 600 and 500 cm^{-1}, two bands are observed and are assigned to the asymmetric deformation modes of PO$_4^{3-}$ group (ν_4). The Raman peak observed at around 400 cm^{-1} is attributed to the symmetric deformation mode (ν_2). The external vibrations give rise to four lines, three of which are very wide. The width of the bands can be explained by the thermal effect.

CONCLUSIONS

In this work, we carried out a study of the powder X ray diffraction and the vibrational spectra of Rb$_3$Ln(PO$_4$)$_2$ phosphates (Ln= La, Ce, Pr, Nd, Sm, Eu, Gd and Tb). The analysis of the spectra allowed us to conclude that these phosphates crystallize in monoclinic system with space group P2$_1$/m by isotypy with K$_3$Nd(PO$_4$)$_2$ compound. The comparison between the Raman and infrared wave numbers shows that the majority of them are not coincident. This confirms that the space group of these phosphates is centrosymmetric.

The attribution of the infrared bands and the Raman lines of these systems is realized in molecular group T$_d$ and factor group C$_{2h}$ on the basis of the bibliographic data.

The comparative study of the vibrational spectra of these compounds shows that the substitution of a rare earth ion by another of smaller size, leads to a shift of the wave numbers to higher values. Consequently, a strengthening of the P–O bonds takes place.

The Rb$_3$Ln(PO$_4$)$_2$ phosphates exhibit a phase transition monoclinic (P2$_1$/m) → trigonal (P-3m1). This phase transition was highlighted by Raman spectroscopy. In fact, the Raman spectrum of Rb$_3$Eu(PO$_4$)$_2$ was recorded at 600°C. This spectrum is very similar to the Raman spectra of K$_2$CsLn(PO$_4$)$_2$ and Rb$_2$CsLn(PO$_4$)$_2$ which have a trigonal structure (P-3m1 space group).The bands observed were attributed by comparison with K$_2$CsLn(PO$_4$)$_2$ and Rb$_2$CsLn(PO$_4$)$_2$ Raman spectra.

REFERENCES

1. M. Kloss, L. Schwarz, J. P. K. Hölsä, *Acta Phys. Polon. A*, **95(3)**, 343 (1999).
2. D. Wisniewski, A. J. Wojtowicz, W. Drozdowski, J. M. Farmer, L. A. Boatner, *J. of Alloys and Compounds*, **380**, 191 (2004).
3. S. V. Ushakov, A. Navrotsky, J. M. Farmer, L. A. Boatner, *J. of Mat. Res.*, **19(7)**, 2165 (2004).
4. J. M. Farmer, L. A. Boatner, B. C. Chakoumakos, C. J. Rawn, D. Mandrus, R. Jin, J. C. Bryan, *J. of Alloys and Compounds*, **588**, 182 (2014).
5. H. B. Tisdale, M. S. Christian, G. Morrison, T. M. Besmann, K. Sun, G. S. Was, H. Loye, *Chem. Mater.*, **34(8)**, 3819(2022).
6. K. V. Ivanovskikh, V. A. Pustovarov, S. Omelkov, M. Kirm, F. Piccinelli, M. Bettinelli, *J. of Lumin.*, **230**, 117749 (2021).
7. A. Pelczarska, A. Watras, P. Godlewska, E. Radominska, L. Macalik, I. Szczgiel, J. Hanuza, P. J. Deren, *New J. of Chemistry*, **39(11)**, 8474 (2015).
8. I. Carrasco, K. Bartosiewicz, F. Piccinelli, M. Nikl, M. Bettinelli, *J. of Lumin.*, **189**, 113 (2017).
9. X. Han, C. Xin, S. Wang, J. Wu, Z. Ye, H. Yu, H. Zhang, *Inorg. Chem.*, **62(24)**, 9679 (2023).

10. S. Ibragimov, F. Ruziev, B. Bobojonov, F. Khudoykulov, *Int. J. of Sci. and Techn. Res*., **9(2)**, 3133 (2020).
11. S. Guo, R. Zhong, K. Gornicka, T. Klimczuk, R. J. Cava, *Chemistry of Mat.*, **32(24)**, 10607 (2020).
12. L. Rghioui, L. Benarafa, M. Saidi Idrissi, A. Lorriaux, F. Wallart, *Spectrochimica Acta Part A*, **52(4)**, 419 (1996).
13. L. Rghioui, R. Nejjar, N. El Jouhari, L. Benarafa, M. Knidiri, A. Lorriaux, F. Wallart, *Can. J. of Anal. Sci. and Spectrosc.*, **43(3)**, 90 (1998).
14. R. Nejjar, L. Rghioui, L. Benarafa, M. Saidi Idrissi, M. Knidiri, *Can. J. of Anal. Sci. and Spectrosc.*, **43(4)**, 107 (1998).
15. L. Rghioui, L. El Ammari, L. Benarafa, M. Knidiri, A. Lorriaux, F. Wallart, H. Krautscheid, *Can. J. of Anal. Sci. and Spectrosc.*, **44(3)**, 86 (1999).
16. L. Rghioui, L. El Ammari, L. Benarafa, J. P. Wignacourt, *Acta Cryst. C*, **58**(7), i90 (2002).
17. L. Benarafa, L. Rghioui, R. Nejjar, M. Saidi Idrissi, M. Knidiri, A. Lorriaux, F. Wallart, *Spectrochimica Acta Part A*, **61(3)**, 419 (2005).
18. L. Rghioui, L. Benarafa, S. Zaydoun, A. Lorriaux, F. Wallart, *Physical and Chemical News*, **31**, 70 (2006).
19. L. Benarafa, L. Rghioui, S. Zaydoun, M. Saidi Idrissi, A. Lorriaux, F. Wallart, *Physical and Chemical News,* **46**, 111 (2009).
20. L. Rghioui, L. Benarafa, J. El Jastimi, A. El Hajji, A. Lorriaux, F. Wallart, *J. of Materials and Environmental Science*, **3(1)**, 57 (2012).
21. L. Rghioui, L. Benarafa, F. Guédira, S. Zaydoun, A. Lorriaux Rubbens, F. Wallart, *J. of Materials and Environmental Science*, **6(11)**, 3015 (2015).
22. L. Rghioui, L. El Ammari, A. Assani, M. Saadi, *Acta Cryst.*, **E75**, 1041 (2019).
23. H. Y.P. Hong, S. R. Chinn, *Mater. Res. Bull.*, **11**, 421 (1976).
24. R. D. Shannon, *Acta Cryst.*, **A32**,751 (1976).
25. W.G. Fateley, F.R. Dolish, N. T. Mc Devit, F. T. Bentley, Infrared and Raman Selection Rules for Molecular and Lattice Vibrations - The Correlation Method, New York, Wiley, 1972.